Synthetic Power Distribution Modeling For Asset Planning

Siavash Hosseini
School of Electrical and Computer Engineering
University of Ottawa
Ottawa, Canada
Siavash.Hosseini@uOttawa.ca

Javad Fattahi
School of Electrical and Computer Engineering
University of Ottawa
Ottawa, Canada
Javad.Fattahi@uOttawa.ca

***Abstract*—This paper introduces a comprehensive methodology for generating synthetic power distribution networks. The proposed framework leverages geospatial data to design cost-effective and operationally robust distribution systems for asset planning that are both geographically consistent and electrically valid. The methodology in this work integrates building coordinates, road networks, and population distributions to determine transformer locations across low, medium, and substation-voltage levels. Low-voltage assets are calculated using constrained clustering to ensure compliance with practical installation and voltage performance criteria. Medium-voltage transformers are assigned through population-balanced regionalization, while substations are obtained from higher-level clustering of MV nodes. Realistic routing is achieved using shortest-path calculations on a municipal street graph, resulting in physically feasible connection layouts. A case study in Ottawa demonstrates how transformer sizing influences cable requirements, voltage performance, and total infrastructure cost. The findings reveal trade-offs between transformer capacity and system expenditure while illustrating the scalability of the proposed approach to large urban regions.**

***Index Terms*—Synthetic Power Distribution, Smart Grid Asset Planning, Transformer Placement.**

I. Introduction

The last twenty years have witnessed exponential growth in power distribution systems, fueled by technological advancements and the growing volume of data produced by intelligent devices [1]. As Industry 4.0 and 5.0 continue to advance, innovative technologies are being deployed to modernize outdated power distribution infrastructure. Key enablers like the Internet of Things (IoT) and cyber-physical systems (CPS) produce vast amounts of sensor data on a daily basis [2]. The integration of these technologies opens new avenues for innovation, driving advancements not only in power distribution networks but across multiple industrial domains. However, evaluating and validating these emerging solutions in real-world scenarios remains constrained by the lack of comprehensive and standardized public test systems. Privacy issues related to network data and insufficient network transparency present substantial barriers to implementing system upgrades and enhancements [2]. Currently, there are a limited number of publicly accessible real-world networks suitable for testing purposes. This scarcity has driven both researchers and industry practitioners to create synthetic test networks that better reflect contemporary distribution systems. Nevertheless, the development of such networks faces significant challenges due to evolving complexities in modern power distribution infrastructures. These include network expansion, incorporation of low-carbon technologies, and high penetration levels of renewable energy sources [3]. Synthetic networks and datasets serve as viable alternatives for testing innovative solutions, allowing researchers to address both the emerging challenges and opportunities in modern power systems. The rapid expansion of power distribution networks, coupled with the integration of low-carbon technologies and renewable energy resources, has heightened the need for synthetic distribution networks and datasets to facilitate testing and innovation. However, existing datasets often lack geographical accuracy, scalability, and regional adaptability, limiting their utility for real-world applications. Several synthetic distribution models rely on Euclidean proximity rather than road-constrained routing, do not explicitly coordinate substation placement under utilization bounds, and can yield unrealistic long-distance aggregation when scaled to city-wide studies.

A Geographical Learner and Generator Algorithm (GLGA) has been developed to create synthetic transmission networks that closely match the structural and spatial properties of a given reference network [4]. The limited availability of geo-referenced distribution network data continues to impede accurate, spatially resolved planning and analysis of modern power systems. Although recent research has introduced methods for the construction of synthetic low- and medium-voltage grids from open data, these approaches often face key limitations, including restrictive topological assumptions, inadequate representation of electrical characteristics, and incomplete integration of real transport infrastructure. Large-scale frameworks, such as those that generate synthetic Swiss MV and LV networks, demonstrate the value of geographically anchored models, but typically rely on load-based clustering or outlier-pruned transport paths and do not explicitly incorporate hierarchical transformer placement, route-based distance constraints, or building-level spatial distributions [5]. These observations motivate synthetic distribution grid models that preserve geographic realism while remaining independent of proprietary utility records.

979-8-3315-8138-1

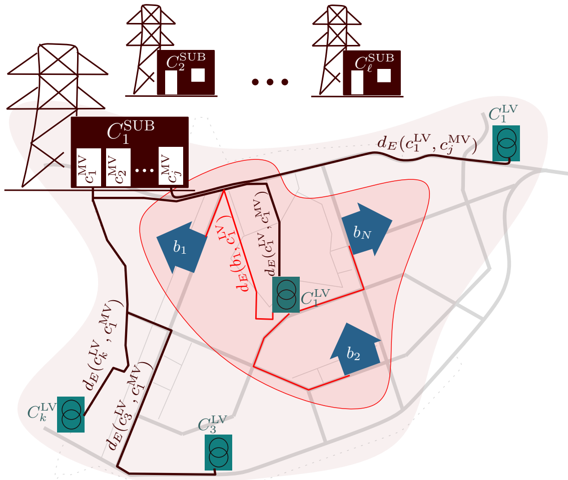

Fig. 1: The proposed hierarchical structure of a synthetic power distribution grid including LV transformers (c_k^{LV}), MV transformers (c_j^{MV}), and substations (c_l^{SUB}), based on building occupancy, geolocation, and population data.

Access to detailed distribution grid data is often limited due to security restrictions, undocumented network changes, and outdated utility records. These limitations make it difficult to analyze existing networks and plan future upgrades. As a result, there is increasing interest in synthetic distribution grid models that can represent real-world networks without relying on confidential data. Furthermore, synthetic grid models are valuable for technology development and utility planning when real network data are unavailable or restricted.

Despite recent progress on synthetic distribution network generation from open geospatial data, practical planning studies still require (i) feeder corridors and wiring distances compatible with real transport infrastructure, (ii) coordinated hierarchical placement and assignment across LV transformers, MV transformers, and substations under explicit capacity bounds, and (iii) scalable mechanisms that prevent unrealistic long-distance aggregation at city scale. The main contributions of this work are: (i) a hierarchical optimization formulation that jointly determines LV transformer, MV transformer, and substation locations and cross-level assignments under explicit capacity and LV route-length constraints; (ii) a road-network-aware routing model that defines building-to-facility and facility-to-facility connection costs using shortest-path distances on an OpenStreetMap-derived weighted graph; and (iii) a scalable solution strategy that mirrors the global formulation through hierarchical clustering, including population-based regionalization to produce realistic MV service areas.

This paper is organized as follows; Section II presents the optimization framework used for hierarchical transformer placement across low-voltage, medium-voltage, and substation levels. Section III presents and highlights the key outcomes of two case studies of a smaller region in downtown Ottawa and then extends the analysis to the entire Ottawa city service area. Finally, Section IV concludes the paper.

II. Methodology

The proposed framework begins with extracting and preprocessing of publicly available geospatial data. Building footprints are obtained from open geospatial datasets, while the underlying road network is extracted from OpenStreetMap. Following this, the synthetic distribution grid is defined over a set of buildings $\mathcal{B} = \{b_1, \dots, b_N\}$, where each building b_i is located at planar coordinates $p_i = (x_i, y_i) \in \mathbb{R}^2$. The road network is modeled as a weighted graph $G = (V, E, w)$, where V is the set of nodes, E is the set of edges, and $w : E \to \mathbb{R}_{>0}$ assigns a positive length to each edge $e \in E$. Each spatial point $p \in \mathbb{R}^2$ (e.g., a building) and each candidate facility location $c \in \mathbb{R}^2$ are associated with their nearest graph nodes $u_p \in V$ and $v_c \in V$, respectively. Let $\mathcal{P}(u, v)$ denote the set of all feasible paths in G connecting nodes $u \in V$ and $v \in V$. Each path $r \in \mathcal{P}(u, v)$ is defined as an ordered sequence of edges, $r = (e_1, e_2, \dots, e_{|r|})$, where each edge $e_k \in E$ can be written as $e_k = (m_k, n_k)$. To ensure that r forms a valid path from u to v, the sequence satisfies the endpoint and continuity constraints $m_1 = u$, $n_{|r|} = v$, and $n_k = m_{k+1}$ for all $k = 1, \dots, |r| - 1$. The route-based distance between two graph nodes u and v is defined as

$$d_{\mathrm{R}}(u, v) = \min_{r \in \mathcal{P}(u,v)} \sum_{e \in r} w(e), \tag{1}$$

and the route-based distance between spatial points p and c is defined as

$$d_{\mathrm{R}}(p, c) = d_{\mathrm{R}}(u_p, v_c). \tag{2}$$

For a given source node u_p, shortest-path distances $d_{\mathrm{R}}(u_p, v)$ to all reachable nodes $v \in V$ are computed using Dijkstra algorithm [6] on the extracted road-network graph. The weight function $w(e)$ is set to the physical length of each road-edge segment $e \in E$. As hypothetically shown in Fig. 1, the network includes three types of facilities. LV transformers are located at $\mathcal{T}_{\mathrm{LV}} = \{c_1^{\mathrm{LV}}, \dots, c_k^{\mathrm{LV}}\}$, MV transformers at $\mathcal{T}_{\mathrm{MV}} = \{c_1^{\mathrm{MV}}, \dots, c_j^{\mathrm{MV}}\}$, and substations at $\mathcal{T}_{\mathrm{SUB}} = \{c_1^{\mathrm{SUB}}, \dots, c_l^{\mathrm{SUB}}\}$. The sets $\mathcal{T}_{\mathrm{LV}}, \mathcal{T}_{\mathrm{MV}}, \mathcal{T}_{\mathrm{SUB}}$ and their elements $c_k^{\mathrm{LV}}, c_j^{\mathrm{MV}}, c_\ell^{\mathrm{SUB}}$ are decision variables representing unknown facility locations to be determined by the optimization.

Each building is supplied by an LV transformer through a mapping $c_{\mathrm{LV}} : \mathcal{B} \to \mathcal{T}_{\mathrm{LV}}$, each LV transformer is connected to one MV feeder via $c_{\mathrm{MV}} : \mathcal{T}_{\mathrm{LV}} \to \mathcal{T}_{\mathrm{MV}}$, and each MV feeder is connected to a substation via $c_{\mathrm{SUB}} : \mathcal{T}_{\mathrm{MV}} \to \mathcal{T}_{\mathrm{SUB}}$. These mappings induce LV, MV, and substation clusters $C_k^{\mathrm{LV}} = \{b_i \in \mathcal{B} : c_{\mathrm{LV}}(b_i) = c_k^{\mathrm{LV}}\}$, $C_j^{\mathrm{MV}} = \{c_k^{\mathrm{LV}} \in \mathcal{T}_{\mathrm{LV}} : c_{\mathrm{MV}}(c_k^{\mathrm{LV}}) = c_j^{\mathrm{MV}}\}$, and $C_\ell^{\mathrm{SUB}} = \{c_j^{\mathrm{MV}} \in \mathcal{T}_{\mathrm{MV}} : c_{\mathrm{SUB}}(c_j^{\mathrm{MV}}) = c_\ell^{\mathrm{SUB}}\}$, which correspond to the LV supply areas, MV feeder groups, and substation service areas, respectively.

The model is governed by capacity parameters $b_{\min}$ and $b_{\max}$ controlling the minimum and maximum number of buildings per LV transformer, and $m_{\min}$ and $m_{\max}$ controlling the minimum and maximum number of MV transformers per substation. These parameters ensure that individual LV

979-8-3315-8138-1

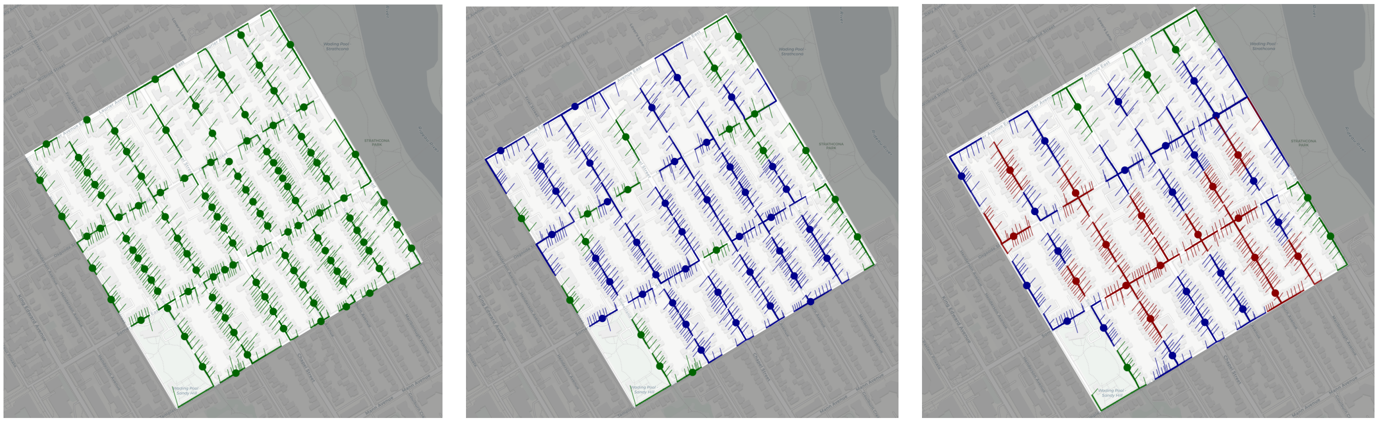

(a) (b) (c)

Fig. 2: Generated transformer networks for case (a) 10 buildings, case (b) 20 buildings, and case (c) 30 buildings. Green clusters represent areas with fewer than 10 buildings supplied by 250-kVA transformers, blue clusters represent areas with up to 20 buildings supplied by 500-kVA transformers, and red clusters represent areas with up to 30 buildings supplied by 750-kVA transformers. Circles indicate the locations of the LV transformers.

transformers and substations are neither overloaded nor underutilized. In the case study, they are selected to correspond to transformer ratings (e.g., up to 10, 20, or 30 buildings mapped to different kVA classes), but they remain symbolic in the formulation. In addition, a route-distance limit $D_{\mathrm{LV}}^{\max}$ is introduced so that building–LV transformer connections respect a maximum LV feeder length consistent with allowable voltage drop at the service level.

Within this framework, the overall routing cost across all levels of the hierarchy is expressed as

$$
\begin{aligned}
D_{\mathrm{total}} = & \sum_{b_i \in \mathcal{B}} d_{\mathrm{R}}(b_i, c_{\mathrm{LV}}(b_i)) \\
& + \sum_{c_k^{\mathrm{LV}} \in \mathcal{T}_{\mathrm{LV}}} d_{\mathrm{R}}\big(c_k^{\mathrm{LV}}, c_{\mathrm{MV}}(c_k^{\mathrm{LV}})\big) \\
& + \sum_{c_j^{\mathrm{MV}} \in \mathcal{T}_{\mathrm{MV}}} d_{\mathrm{R}}\big(c_j^{\mathrm{MV}}, c_{\mathrm{SUB}}(c_j^{\mathrm{MV}})\big)\,,
\end{aligned} \tag{3}
$$

where the first term accounts for building–LV connections, the second for LV–MV connections, and the third for MV–substation connections. This quantity aggregates the route-based wiring distances that must be constructed in the final network, and thus serves as the primary objective of the design. The synthetic network design problem is then posed as the constrained optimization

$$
\begin{aligned}
\min_{\substack{\mathcal{T}_{\mathrm{LV}}, \mathcal{T}_{\mathrm{MV}}, \mathcal{T}_{\mathrm{SUB}}, \\ c_{\mathrm{LV}}, c_{\mathrm{MV}}, c_{\mathrm{SUB}}}} \quad & D_{\mathrm{total}} \\
\text{s.t.} \quad & b_{\min} \le |C_k^{\mathrm{LV}}| \le b_{\max}, \quad \forall\, k, \\
& m_{\min} \le |C_\ell^{\mathrm{SUB}}| \le m_{\max}, \quad \forall\, \ell, \\
& d_{\mathrm{R}}(p_i, c_{\mathrm{LV}}(b_i)) \le D_{\mathrm{LV}}^{\max}, \quad \forall\, b_i \in \mathcal{B},
\end{aligned} \tag{4}
$$

where the clusters $C_k^{\mathrm{LV}}, C_j^{\mathrm{MV}}, C_\ell^{\mathrm{SUB}}$ are implicitly defined by the assignment mappings. Problem (4) compactly encodes the hierarchical clustering and routing structure: LV, MV, and substation locations are chosen, buildings and transformers are assigned across levels, and the resulting network must satisfy capacity and distance constraints while minimizing the total route-based distance (3).

In implementation, this global problem is solved hierarchically using Euclidean clustering objectives that mirror classical k-means formulations. The Euclidean distance between two points p and q is defined as $d_{\mathrm{E}}(p, q) = \|p - q\|_2$. At the LV level, buildings p_i are grouped into LV clusters C_k^{LV} and centroids c_k^{LV} by minimizing the sum of squared Euclidean distances

$$
\sum_{k=1}^{K_{\mathrm{LV}}} \sum_{b_i \in C_k^{\mathrm{LV}}} d_{\mathrm{E}}\big(p_i, c_k^{\mathrm{LV}}\big)^2, \tag{5}
$$

subject to the LV capacity and route-distance constraints described above. This step yields LV transformer locations that are spatially representative of nearby buildings while ensuring that all buildings remain within an acceptable feeder distance along the road network.

To incorporate population density, the study area is partitioned into regions $R_1, \ldots, R_M$, each having approximately $\mathrm{Population}(R_m) \approx P_{\mathrm{reg}}$ for a chosen design parameter P_{reg} (e.g., $4{,}000$ residents). Within each region R_m, the LV transformers that lie in the region form a subset $\mathcal{T}_{\mathrm{LV}}^{(m)} \subseteq \mathcal{T}_{\mathrm{LV}}$. These regional LV transformers are then clustered into MV service areas by minimizing, for each region,

$$
\sum_{j=1}^{K_{\mathrm{MV}}^{(m)}} \sum_{c_k^{\mathrm{LV}} \in C_j^{\mathrm{MV}(m)}} d_{\mathrm{E}}\big(c_k^{\mathrm{LV}}, c_j^{\mathrm{MV}(m)}\big)^2, \tag{6}
$$

where $C_j^{\mathrm{MV}(m)}$ denotes the set of LV transformers assigned to the j-th MV transformer in region R_m, and $c_j^{\mathrm{MV}(m)}$ is its location. This regional clustering guarantees that MV transformers naturally align with population-based service areas, preventing unrealistic long-distance aggregation of LV clusters.

Finally, all MV transformer locations are grouped into substation service areas by clustering $\mathcal{T}_{\mathrm{MV}}$ into substation

979-8-3315-8138-1

clusters C_ℓ^{SUB} with centroids c_ℓ^{SUB}, again using a squared Euclidean objective of the form

$$\sum_{\ell=1}^{K_{\mathrm{SUB}}} \sum_{c_j^{\mathrm{MV}} \in C_\ell^{\mathrm{SUB}}} d_{\mathrm{E}}\big(c_j^{\mathrm{MV}}, c_\ell^{\mathrm{SUB}}\big)^2, \tag{7}$$

subject to the substation capacity constraints. This step determines substation locations that are centrally located with respect to the MV transformer population they serve.

III. Case Study

This study initially focuses on a localized area in Ottawa, considering transformer capacities corresponding to 10, 20, and 30 buildings, where a 250-kVA transformer is used to serve 10 buildings, and the 20 and 30-building cases are mapped to 500-kVA and 750-kVA transformers, respectively, to assess the framework's operational feasibility. For the optimization model, these scenarios correspond to different choices of the LV capacity parameters $b_{\min}$ and $b_{\max}$ in (4), which control the feasible range of cluster sizes $|C_k^{\mathrm{LV}}|$. Subsequently, the analysis is extended to the Ottawa city region to show the scalability of the proposed methodology in a larger and more complex urban environment. The methodology consists of the following main stages: (i) building data extraction, (ii) optimal placement of low-voltage transformers using the LV clustering objective (5), (iii) determination of the best connection routes between buildings and transformers under the predefined distance constraints in Section II and the route-based distance definition (2), (iv) assignment of medium-voltage transformers according to each region's population via the MV objective (6), and (v) assigning substations for every 8 to 20 MV transformers using the substation clustering objective (7) and the capacity bounds in (4).

In the first step, 765 building coordinates were extracted for the designated study area in Ottawa. Subsequently, an optimization algorithm was applied to determine the optimal locations of LV transformer centroids using the objective in (5), ensuring that each cluster of buildings is served efficiently while satisfying transformer capacity constraints and adhering to urban development patterns. In this local case, the parameters $b_{\min}$ and $b_{\max}$ in (4) are chosen to reflect the desired transformer loading in terms of the number of buildings per LV unit. After assigning buildings to their respective transformer centroids, the proposed method identifies the optimal connection routes $r_i^\star$ between each building b_i and its assigned centroid c_k by solving the shortest-path problem induced by the route-based distance $d_{\mathrm{R}}(\cdot,\cdot)$ in (2) on the distance-weighted road network graph $G = (V, E, w)$. These routes are computed using existing road data to ensure that the resulting distribution network is both geographically and physically realistic, and they directly contribute to the building–LV component of the global routing cost in (3).

The optimization minimizes the total route-based distance between buildings and their assigned transformers as captured by the first term in the global objective (3), while imposing practical constraints such as limiting maximum line lengths via the bounds $D_{\mathrm{LV}}^{\max}$ and $D_{\max}$ in (4) and maintaining consistency with existing infrastructure. In certain cases, the algorithm may not select the visually shortest path between a building and a transformer when viewed on a map, due to the fact that the feasible path set $\mathcal{P}(u_i, v_k)$ in (2) excludes unavailable or unmapped road segments. Consequently, such visually shorter but inaccessible routes are not considered in the computation of $r_i^\star$, and the effective connection distance is given by the network-compatible path length $d_{\mathrm{R}}(p_i, c_k)$.

TABLE I: Comparison of the configurations and costs for the three scenarios.

Metric	**Case (a)**	**Case (b)**	**Case (c)**
Number of 250-kVA transformers	108	18	6
Number of 500-kVA transformers	0	41	21
Number of 750-kVA transformers	0	0	16
Maximum wiring length (m)	134.8	143.7	144.1
Average wiring length (m)	12.48	24.01	32.26
Maximum voltage drop (%)	5.2	11.1	16.6
Average voltage drop (%)	0.48	1.85	3.73
Total wiring length (m)	7098	13479	14050
Overall wiring cost (CAD)	**127,764**	**242,622**	**252,900**
Overall transformer cost (CAD)	**8,100,000**	**6,270,000**	**5,530,000**
Overall system cost (CAD)	**8,227,764**	**6,512,622**	**5,782,900**

For the Ottawa city case study, as illustrated in Fig. 3, the framework is applied to $N = 246{,}097$ buildings in the service area. Buildings are modeled as elements of $\mathcal{B}$ with coordinates (x_i, y_i) and grouped into LV clusters C_k^{LV} using (5). In this large-scale scenario, the parameters are set to $b_{\min} = 7$ and $b_{\max} = 30$ for all LV clusters. The solution of (5) under these constraints yields the LV transformer locations c_k^{LV} for the entire building set. Correspondingly, the MV layer is formed by aggregating LV centroids within population-defined regions and solving (6) to obtain MV transformer locations c_j^{MV}. Substations are then placed by clustering MV sites under the capacity bounds $8 \le |C_\ell^{\mathrm{SUB}}| \le 20$, corresponding to the parameters $m_{\min} = 8$ and $m_{\max} = 20$ in (4), and solving (7) for substation centroids c_ℓ^{SUB}. All connections between buildings, LV transformers, MV transformers, and substations are routed along the road network using the shortest-path formulation in (2), and the overall routing effort across all hierarchy levels is measured by the global objective (3). These hierarchical decisions are coordinated through the constrained optimization problem in (4), which is evaluated over the full set of 246,097 buildings to obtain a scalable synthetic network for the Ottawa city region.

The proposed methodology, formulated as the hierarchical optimization problem in (4) with objective (3) and route-based distance definition (2), was implemented within a selected urban area of Ottawa, resulting in the generation of a synthetic distribution network. Fig. 2 demonstrates the effect of transformer capacity constraints on the clustering and routing structure of the synthetic distribution network.

The defined capacity and distance constraints in the optimization framework (4) played a vital role in ensuring that transformer loads remained within permissible limits and that LV feeder lengths respected the design bounds. In particular, the LV and substation capacity limits $b_{\min}, b_{\max}, m_{\min}, m_{\max}$ and the route-distance thresholds $D_{\mathrm{LV}}^{\max}$ and $D_{\max}$ appearing in

979-8-3315-8138-1

Fig. 3: Synthetic power distribution grid generated for Ottawa city service area. For visualization, the map is rotated by -20° to improve horizontal allignment.

(4) directly restrict the feasible assignments between buildings, LV transformers, MV transformers, and substations. This adherence to the constraints in (4) directly validates the electrical plausibility of the synthetic network design, confirming its viability for real-world applications.

The results in Table I illustrate the impact of varying transformer capacities (encoded through the parameters $b_{\min}, b_{\max}, m_{\min}, m_{\max}$ in (4)) on key network parameters, including infrastructure requirements and associated costs. The cost analysis assumes that low-voltage distribution wiring is installed using 1/0 AWG all-aluminum conductor (AAC) cable at a market price of CAD $18 per meter, consistent with typical pricing from Canadian electrical suppliers. Transformer costs were assigned using representative commercial prices for three-phase pad-mounted distribution units: CAD $75,000 for a 250-kVA transformer, CAD $120,000 for a 500-kVA transformer, and CAD $160,000 for a 750-kVA transformer. These values were used to calculate the total wiring, transformer, and overall system cost for each scenario, based on the network layout produced by solving (4) and the resulting routing distances in (3). Voltage drop, another essential component of the analysis, is implicitly controlled through the LV feeder distance limit $D_{\mathrm{LV}}^{\max}$ and the global bound $D_{\max}$ in (4), and is a key determinant of the electrical feasibility and operational reliability of distribution networks, as excessive drop can lead to equipment malfunction, energy losses, and regulatory non-compliance.Accurate voltage drop analysis helps choose proper conductor sizes, place transformers effectively, and design the overall network layout. This improves energy efficiency, reduces costs, and ensures compliance with power quality standards. In synthetic network generation, voltage drop evaluation also confirms that spatially optimized designs are electrically reliable and practically feasible [7].

While the proposed methodology demonstrates strong alignment with real distribution grid constraints and requirements, it can be enhanced by post-validation through time-series load, EV, and DER injections together with downstream control actions (inverter Volt/VAR setpoints, regulator/capacitor operations, and switching actions), followed by distribution power flow. Such validation can quantify feasibility metrics including voltage compliance, thermal loading, and unbalance indices, and can support tuning of the synthetic grid under corrective controls for long-term planning.

IV. Conclusion

We presented an approach for generating synthetic power distribution networks. This framework generated transformer configurations that adhered to routing and voltage constraints while reflecting realistic urban layouts. The analysis of three capacity scenarios, 10 buildings per 250-kVA transformer, 20 buildings per 500-kVA transformer, and 30 buildings per 750-kVA transformer, demonstrated how asset sizing directly shapes infrastructure requirements. The voltage drop followed similar trends, with maximum drops rising from 5.2% to 16.6% as the cluster size and transformer rating increased, underscoring the trade-off between cost and power quality.

Acknowledgment

Portions of this manuscript were grammar-checked using AI tools. All technical content, analyses, and conclusions were conceived, developed, and validated solely by the authors.

References

[1] P. K. R. Maddikunta, Q.-V. Pham, B. Prabadevi, N. Deepa, K. Dev, T. R. Gadekallu, R. Ruby, and M. Liyanage, "Industry 5.0: A survey on enabling technologies and potential applications," *Journal of industrial information integration*, vol. 26, p. 100257, 2022.

[2] M. Ali, K. Prakash, C. Macana, M. Raza, A. K. Bashir, and H. Pota, "Modeling synthetic power distribution network and datasets with industrial validation," *Journal of Industrial Information Integration*, vol. 31, p. 100407, 2023.

[3] S. Li, S. Wang, Q. Zhao, D. Liu, and C. Tse, "A risk assessment framework for large-scale synthetic power distribution networks considering historical hurricane disasters," *IEEE Transactions on Power Systems*, 2025.

[4] B. Abhilash, C. Syranidou, J. Linssen, and D. Stolten, "Geo-referenced synthetic low-voltage distribution networks: A data-driven approach," in *2021 IEEE PES Innovative Smart Grid Technologies Europe (ISGT Europe)*, pp. 1–6, IEEE, 2021.

[5] A. Oneto, B. Gjorgiev, F. Tettamanti, and G. Sansavini, "Large-scale generation of geo-referenced power distribution grids from open data with load clustering," *Sustainable Energy, Grids and Networks*, vol. 42, p. 101678, 2025.

[6] E. W. Dijkstra, "A note on two problems in connexion with graphs," *Numerische Mathematik*, vol. 1, pp. 269–271, 1959.

[7] I. S. Islahuzzaman, M. I. Sudrajat, N. Moonen, J. Popovic, and F. Leferink, "The significance of cable and nonlinear loads to losses, voltage drop, and harmonics in remote off-grid systems," *IEEE Letters on Electromagnetic Compatibility Practice and Applications*, vol. 6, no. 2, pp. 72–78, 2024.

979-8-3315-8138-1